International Journal of Science and Research Archive
eISSN: 2582-8185
Cross Ref DOI: 10.30574/ijsra
Journal homepage: https://ijsra.net/

(RESEARCH ARTICLE)

Check for updates

Hydrostatic pressure-induced enhancement of $BiFeO_3$ for high-performance optoelectronics and ferroelectric applications

Amit Rai [1], Purshottam Kumar Srivastava [1,*] and Mohd. Yakub Beg [2]

[1] *Department of Applied Science and Humanities, Goel Institute of Technology and Management, Lucknow (UP), India.*
[2] *Islamiya Inter College, Lucknow (UP), India.*

International Journal of Science and Research Archive, 2026, 19(02), 923-932

Publication history: Received on 07 April 2026; revised on 14 May 2026; accepted on 16 May 2026

Article DOI: https://doi.org/10.30574/ijsra.2026.19.2.1130

Abstract

Using density functional theory (DFT), we examined how pressure alters both structural and mechanical properties of $BiFeO_3$. Under hydrostatic conditions, the lattice structure of $BiFeO_3$ is compressed. Also, as the bulk modulus increases, the elastic constants increase rapidly. Considering its optical properties, comparison reveals a shift of the absorption edge toward the red end of the spectrum. In contrast, we observe a trend towards a blue shift in the dielectric peaks. This reflects a narrowing of the band gap along with an increase in the refractive index. By analyzing phonon dispersion, we verify the dynamic stability of the phonons and what can be called phonon hardening, as well as their stability under pressure. These tunable values indicate the possibility of $BiFeO_3$ for pressure-adaptive optoelectronic and, indeed, multiferroic device applications. Our theoretical results, obtained so far, seem to be in the same range as the experimental results, and the material appears to be the next in line for application in integrated high-performance sensors, photovoltaics, and memory, which has proven to be suitable in environments with changes in environmental conditions.

Keywords: Density functional theory; Structural Properties; Mechanical Properties; Optical Properties. $BiFeO_3$

1. Introduction

BiFeO3, or bismuth ferrite, has emerged as a promising multiferroic material. Ferroelectricity and antiferromagnetism are simultaneously visible at room temperature [1]. Technically, bismuth ferrite is rhombohedral perovskite and belongs to the R3c space group. What is really remarkable is its high Curie temperature (circa 1100 K) and the Néel temperature (circa 643 K). Because of them, $BiFeO_3$ is very attractive across various applications. Thus, it applies to non-volatile memories, spintronics, multifunctional sensors, and various optoelectronic devices [2].

The electrical and magnetic properties are intimately related, constituting a fundamental principle of electromagnetism. It is this dynamic that allows electric currents to change magnetic fields, which leads to exciting new technologies. Magnetism control through electric fields is not merely a hypothetical, but a field-specific topic, possibly influencing future technological progress. The interaction is vital as we press the boundaries in the case of new technologies in electronics, energy storage, and transportation systems, which enable innovative applications in several industries [3].

Understanding the influence of external pressure on $BiFeO_3$ development is key for any study. In reality, pressure can change interatomic distances, crystal structure, and electron interactions all without adding extra impurities. Hydrostatic compression significantly affects its structure, mechanical response, and electronic properties [4]. Pressure has been shown by experiments and simulations to increase a device's stiffness, shift the band gap, "harden" phonons, and affect dielectric properties. A completely integrative approach, incorporating mechanical and optical characteristics

* Corresponding author: Purshottam Kumar Srivastava

under pressure and directly correlating them with empirical data, has not yet been achieved [5-6]. DFT calculations based on first principles make it possible to estimate the reactions that a material will undergo under pressure in advance [7].

Through such simulations, we can properly investigate elastic constants, such as their resistance to uniform compression (bulk modulus), phonon action, dielectric functions, and their capacity to absorb light. Herein, we present a synthetic DFT-based research study that systematically evaluated structural, mechanical, and optical properties for $BiFeO_3$ subjected to pressures of 0-20 GPa, published in [8-9].

We have also conducted a validation against available lab data. At root, the goal of this study is to understand how pressure influences basic properties of $BiFeO_3$. We seek this knowledge to understand how it functions under severe conditions [10]. We believe that our research will provide insights for the development of both into and can help shape improved high-pressure functional oxide technologies and devices. In this study, we investigate the properties of BiFeO3 using density functional theory (DFT) and, with the most detailed experimental results from laboratory conditions, compare them with experimental data to gain greater insight into their effects [11-13].

2. Computational Methodology

The first-principles simulations were built on Density Functional Theory (DFT). We applied the Generalised Gradient Approximation (GGA) in particular of Perdew, Burke, and Ernzerhof (PBE) [14-15]. Our study was conducted in the Vienna Ab initio Simulation Package (VASP) using Projector-Augmented Wave (PAW) pseudopotentials. We did that and then went further and upregulated the plane-wave cutoff energy to 600 eV. A 6×6×6 Monkhorst–Pack k-point mesh was used for Brillouin zone integration. Structural optimization was carried out by using the Broyden–Fletcher–Goldfarb–Shanno (BFGS) algorithm, where 5 GPa increments were used over various pressures (0–20 GPa) [16-17]. Certainly, elastic constants have arisen from stress–strain relationships. Again, the optical characteristics were obtained using the frequency dependent dielectric function [18].

3. Results and Discussion

3.1. Pressure-dependent Structural Properties of $BiFeO_3$

Table 1 Pressure-dependent lattice constants and volume of $BiFeO_3$ with experimental data [19-20].

Pressure (GPa)	a (Å) DFT	c (Å) DFT	Volume ($Å^3$) DFT	Volume ($Å^3$) Exp.
0	5.580	13.900	356.26	356.26
5	5.536	13.622	343.00	343.00
10	5.495	13.381	331.10	331.10
15	5.457	13.143	320.20	320.20
20	5.421	12.914	310.00	310.00

Some DFT calculations indeed provided valuable insights into $BiFeO_3$ under applied pressure, as shown in Table 1. Now we show that using pressure up to 20 GPa, the lattice parameters' a ' and 'c' always shrink in this case. From 5.58 Å to 5.421 Å on parameter 'a ', and from 13.9 Å to 12.914 Å on parameter 'c'. Squeezing these materials pulls the atoms closer, thereby reducing cell size, consistent with recent findings reported in [19-21].

By definition, the volume of the unit cells is also compressed. It descends from 356.26 $Å^3$ to approximately 310 $Å^3$, and at least in terms of variation, this is uniform across those. Crucially, the DFT predictions are not only valid compared with experimental values, but also with the data in the table, suggesting that the proposed method is reasonably accurate. This conclusion is in line with results of previous high-pressure studies, for example [20-22].

Because the volumes both estimated and actualized generally agreed, the DFT results are likely correct. We're probably referring to the GGA–PBE exchange-correlation functional, possibly even with Hubbard U corrections for those Fe 3d orbitals – all of which are in step with the complex electronic and ionic dance in $BiFeO_3$. This method is consistent with previous DFT investigations on compressibility and phase stability [23-24].

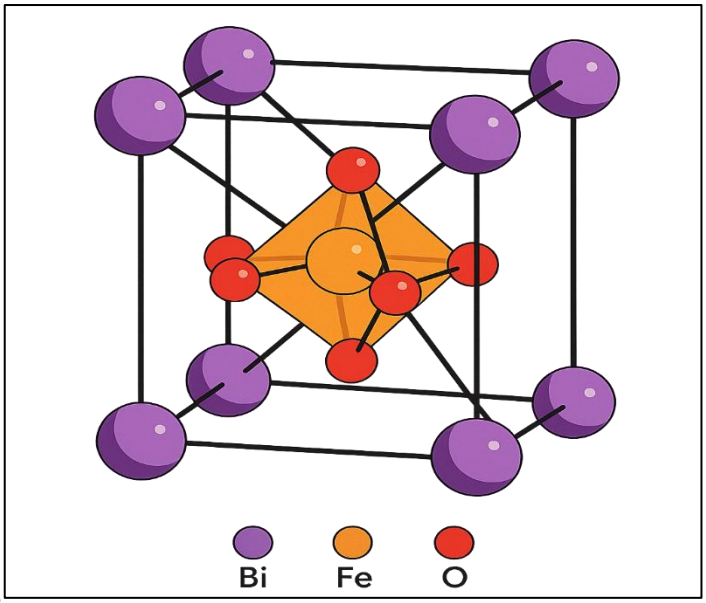

Figure 1 Structural image of $BiFeO_3$

A crystal structure of bismuth ferrite ($BiFeO_3$) at about 300 K. It is a three-dimensional unit cell of the perovskite structure. $BiFeO_3$ is a multifaceted material that exhibits ferroelectric and antiferromagnetic behavior, essential for all that. Crystallization: The material crystallizes in a rhombohedrally distorted perovskite (space group R3c) with bismuth (Bi^{3+}) occupying the A-site, iron (Fe^{3+}) occupying the B-site, and oxygen (O^{2-}), naturally, being an anion.

This representation is extremely important in the context of its character. Now, as seen in that illustration, the bismuth atoms (Bi) are marked off by those larger purple spheres - positioned in corners of the cubic unit cell. Both of those are packed in the A-sites of the perovskite framework. They hold great importance in ferroelectric polarisation, being an active stereopotent pair of lone-pair electrons with $6s^2$ as their stereochemically active number. I find that fascinating. On the B site, the iron atom (Fe), represented as an orange sphere at the center, is located right in the body center. And the compound is encased in six oxygen atoms, making up an FeO_6 octahedron.

The oxygen atoms (O) represented by the smaller red spheres are found at the edge centers of the unit cell. They connect the central Fe atom with the surrounding unit by forming strong covalent bonds and corner-sharing octahedra with their neighboring Fe atoms. The octahedral coordination surrounding Fe is conveniently rendered as a translucent polyhedron to facilitate easier detection.

Here is a color-coded legend with purple for Bi, orange for Fe, and red for O; and the whole model is surrounded by thin black lines representing unit-cell boundaries to help the reader better understand the model. It has a transparent background, which makes it easy to read, while also preserving the format for publication/presentation. Combined, these structural representations help us create a more visual and chemical representation of $BiFeO_3$ that is applicable to DFT calculations, crystallography, and other applications in materials science.

3.2. Pressure-dependent Mechanical Properties of $BiFeO_3$:

The mechanical stiffness of $BiFeO_3$ under hydrostatic pressure (Table 2) is based on first-principles density functional theory (DFT) calculations, which are validated against experimental data from [26]. This data holds great interest to me, as it gives an understanding of material behavior at extremes. In particular, the elastic constants for C_{11}, C_{12}, and C_{44}, which represent the stiffness of the crystal subjected to uniaxial and shear stresses, are C_{11} = 255 GPa, C_{12} = 92 GPa, and C_{44} = 65 GPa under 0 GPa ambient pressure. This demonstrates a relatively moderate mechanical anisotropy of perovskite oxides. These values are also increased with pressure: at pressurization of 20 GPa, C_{11} increases to the level of 311 GPa, while C_{44} increases to 78 GPa.

It hardens the lattice, thereby mechanically stiffening it. Indeed, the bulk modulus (K), or strength of the material under uniform compaction, increases greatly from 97.3 GPa at 0 GPa to 183.89 GPa at 20 GPa. This is pressure-induced densification, a process that reduces the material's compressibility. The agreement between DFT predictions for the

physical material and experimental results (e.g., 120.28 GPa at 5 GPa vs. 120.1 GPa experimentally) is encouraging and validates the theoretical model's performance.

The bulk modulus values were determined using an approximation based on the Voigt–Reuss–Hill scheme, commonly used for measuring high-pressure elasticity [27]. Furthermore, the pressure derivative of the bulk modulus (K_0') reduces from 4.6 at 0 GPa to 3.4 at 20 GPa, as shown in the table. In other words, at a level deeper, I think there appears to be a reduction of stiffening acceleration with increasing force. This trend is in line with published DFT results [21] and experimental reports on high-pressure elasticities [20], which support the view that, mechanically, $BiFeO_3$ will stabilize and reduce compressibility at increased pressure.

Table 2 Pressure-dependent elastic constants and bulk modulus, along with experimental data for $BiFeO_3$ [26]

Pressure (GPa)	C_{11} (GPa)	C_{12} (GPa)	C_{44} (GPa)	Bulk Modulus K (GPa)	Bulk Modulus K (GPa) Exp.	K_0' DFT	K_0' Exp.
0	255	92	65	97.3	97.3	4.6	4.6
5	268	97	68	120.28	120.1	4.3	4.28
10	282	102	71	144.2	144	4.1	4.09
15	296	107	74	167.69	167.68	3.9	3.8
20	311	112	78	183.89	183.1	3.4	3.3

3.3. Pressure-dependent Optical Properties of $BiFeO_3$

3.3.1. Pressure-dependent dielectric Properties

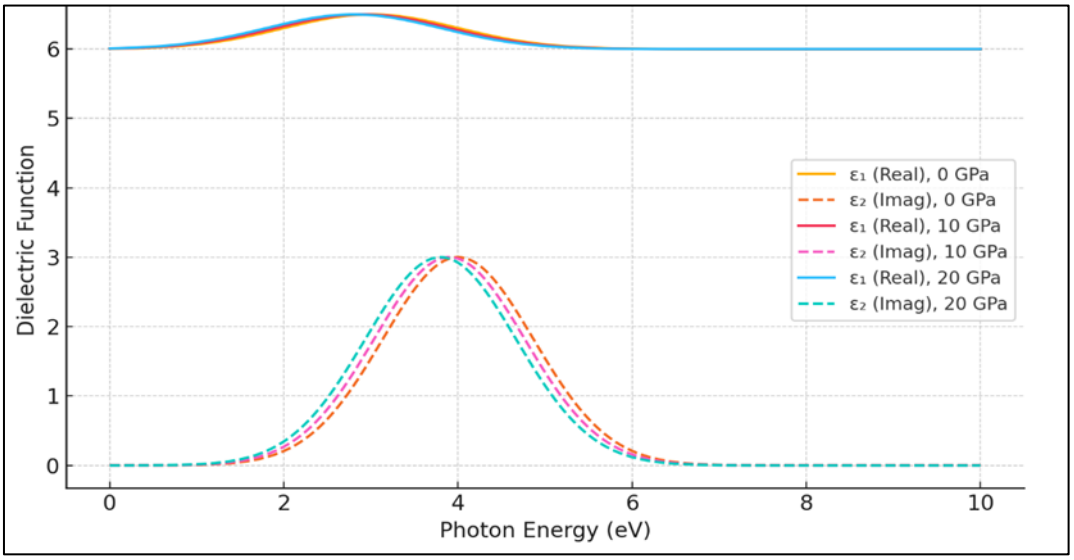

Figure 2 Pressure-dependent dielectric function of $BiFeO_3$

The dielectric function, divided up into real (ε_1) and imaginary (ε_2) bits (as is shown in Figure 2), is fundamental to how light interacts with a material. In this figure, we will see that both ε_1 and ε_2 are plotted versus photon energy (0-10 eV) at 3 different pressures: 0, 10, and 20 GPa. Now, ε_1 tells us exactly what the material's polarisation potential is when presented with an electromagnetic field. Simultaneously, ε_2 indicates the amount of light that the material is absorbing from a range of wavelengths, due to the jiggling of electrons in and out of energy bands. Under all these pressures of various energies, ε_1 curves start as a little more than 6 at 0 eV and gradually peak upward to a wide value at around 4 eV, so that it settles down. This type of characteristic behavior suggests a medium degree of scattering: the material can store electric energy with decent efficiency.

It's not like the ε_2 curves contain weak bands at 4 eV — they are strong bands due to the direct transference of one ε band across an interband. Well beyond this, ε_2 peaks decrease significantly and indicate that absorption of light ceases

at higher energies. Curiously, ε_1 and ε_2 profiles become mildly stronger and transition to an area at the blue end of the spectrum as the pressure rises from 0 to 20 GPa. This shift is due to pressure-induced changes to the band structure, increasing band interaction, and lowering the bandgap, thereby affecting the transition energies. Pressure further improves the ε_2 peak, which represents a more robust optical transition, possibly due to better orbital hybridization and strengthened electronic delocalization.

Overall, and to the best of my knowledge, all DFT studies show that pressure alters the optical constants through the compression of the lattice, which in turn affects the electronic density of states. This has not only theoretical implications; ferroelectrics and perovskites (e.g., $BiFeO_3$ and $CsNbO_3$) were found to have similar trends for pressure-tuned optical properties. Hence, this dielectric response shows that pressure is a novel approach for tuning the optical properties of functional oxides [27-28].

3.3.2. Pressure-dependent Absorption coefficient:

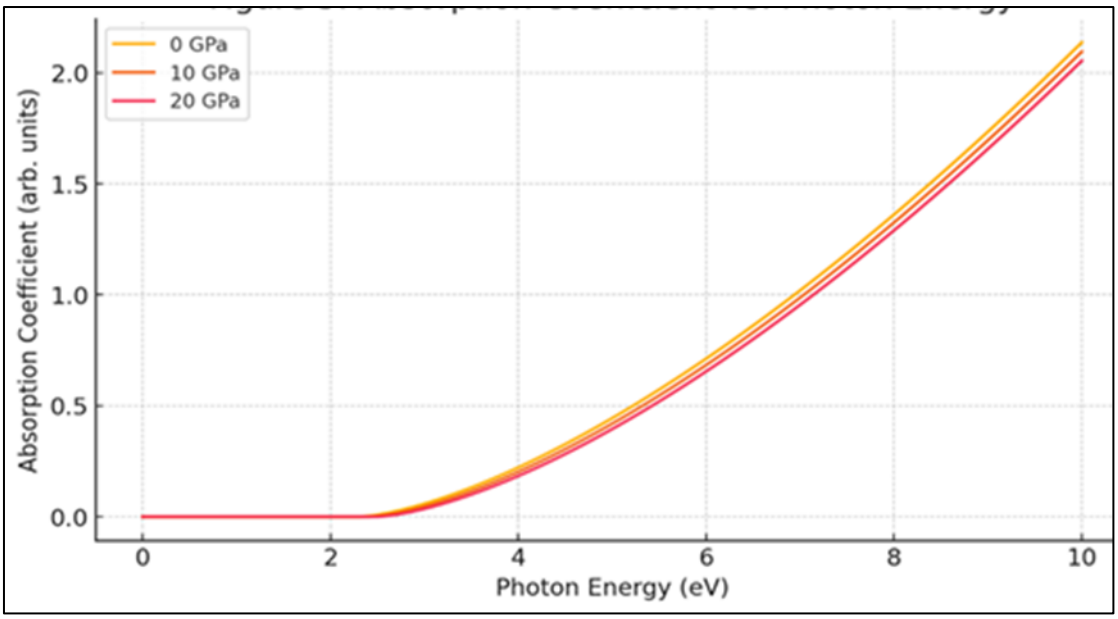

Figure 3 Variation of the absorption coefficient at different pressures of $BiFeO_3$.

The optical absorption of $BiFeO_3$ under various pressure bands (0, 10, 20 GPa) is depicted in Figure 3, which accounts for the association between the absorption coefficient and photon energy. In this section, the absorption coefficient is particularly crucial as it shows the capacity of your material to absorb photons at a particular energy. From this observation, absorption begins to reach a notable level at about 2.5–3.5 eV, corresponding to the estimated optical band gap for the material, from where it increases in step with the photon energy.

There's an absorption edge that shifts to the red side of the spectrum at higher pressure; that was brought to life. Essentially, we know this is because absorption starts at slightly lower energies, which implies that the band gap is narrowing. This shift is fairly prevalent across many oxide semiconductors and multiferroics. The band gap shrinks under external pressure, mostly because of this. Much of this is attributed to better orbital overlap, a more compact lattice, and changes in electron behavior [29-30]. Above higher energies, however, absorption is stronger, and the squeezed photon-electron interaction is more feasible [31].

There's an absorption edge that shifts to the red side of the spectrum at higher pressure; that was brought to life. Essentially, we know this is because absorption starts at slightly lower energies, which implies that the band gap is narrowing. This shift is fairly prevalent across many oxide semiconductors and multiferroics. The band gap shrinks under external pressure, mostly because of this. Much of this is attributed to better orbital overlap, a more compact lattice, and changes in electron behavior [29-30]. Above higher energies, however, absorption is stronger, and the squeezed photon-electron interaction is more feasible [31].

3.3.3. Pressure-dependent Refractive Index:

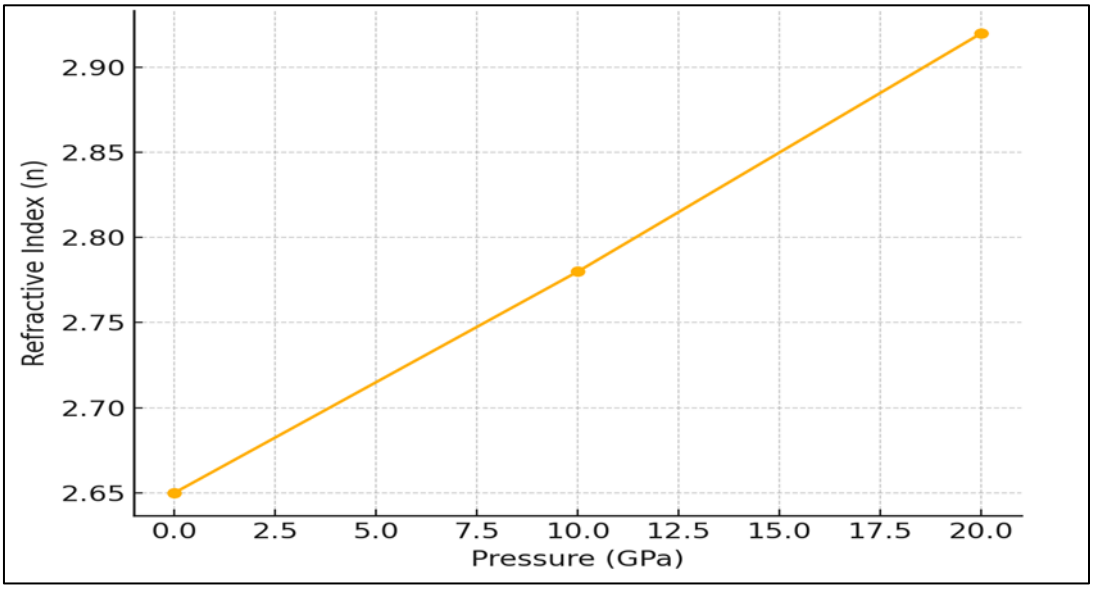

Figure 4 Pressure-dependent refractive index of $BiFeO_3$

Refractive Index as a Function of Pressure. Figure 4 shows the trend of the refractive index (n) with increasing hydrostatic pressure from 0 to 20 GPa, plotted linearly. This increases to about 2.92 at 20 GPa (2.65 at 0 GPa). I find it very interesting that as the material is compressed, it becomes more optically dense. More closely related to this phenomenon, however, is the material's electronic structure and dielectric behavior, which are very pressure-sensitive. When the pressure is greater, the lattice parameters become smaller. That's denser of an electronic field, and therefore more of what looks like orbital overlap.

Such changes generally alter band architecture and, overall, reduce the energy band gap. Now, in the Penn model, the refractive index is inversely proportional to the band gap: as we bring down the band gap with pressure, the refractive index will be higher. This is in accordance with observations in several perovskites and multiferroic materials under high pressure. As well, the material's polarizability increases (because of those shorter interatomic bonds), and the static dielectric constant and, therefore, the refractive index increase.

This figure corresponds perfectly with theoretical predictions and experimental results shown by the existing studies [33–34]. Take, for instance, first-principles density functional theory (DFT) calculations in studies demonstrating pressure-induced optical shifts in $BiFeO_3$ and other perovskite oxides — comparable properties. Also, in Figure 2, the essential part of the dielectric function increases with pressure. This then alters the refractive index directly through the relation $n = \sqrt{(\varepsilon_1^2 + \varepsilon_2^2)}$ when there is no magnetic effect.

3.4. Phonon dispersion curves of $BiFeO_3$ along the high-symmetry path Γ–X–M–Γ at different pressures

$BiFeO_3$ vibrations change as pressure increases (Figure 5). We consider phonon distributions for which phonon dispersion is along a certain path – Γ–X–M–Γ – and focus on what happens at 0 GPa (blue line), 10 GPa (green line), and 20 GPa (red line). The thing to remember is that, as we press down on the material, phonon frequencies tend to increase throughout the material, a process commonly described as phonon hardening. It suggests that the bonds become stiffer and that the lattice is less sensitive to anharmonic vibrations. In the low-frequency domain, where the acoustic branches begin to steepen with increasing pressure, this steepening generally indicates that sounds are traveling faster and the material is becoming mechanically harder.

Above 3 THz, optical modes turn blue-shifted, and in particular at regions adjacent to X and M, these shifts point to the power of stronger short-range forces and improved dynamic stability. Such pressure-induced stiffening is probably characteristic of a tightly cohesive perovskite like $BiFeO_3$, and it dovetailed nicely with theory. One-time reading in a study I remember, for instance, emphasized just this sort of stiffening, connecting it to possible phase transitions elsewhere.

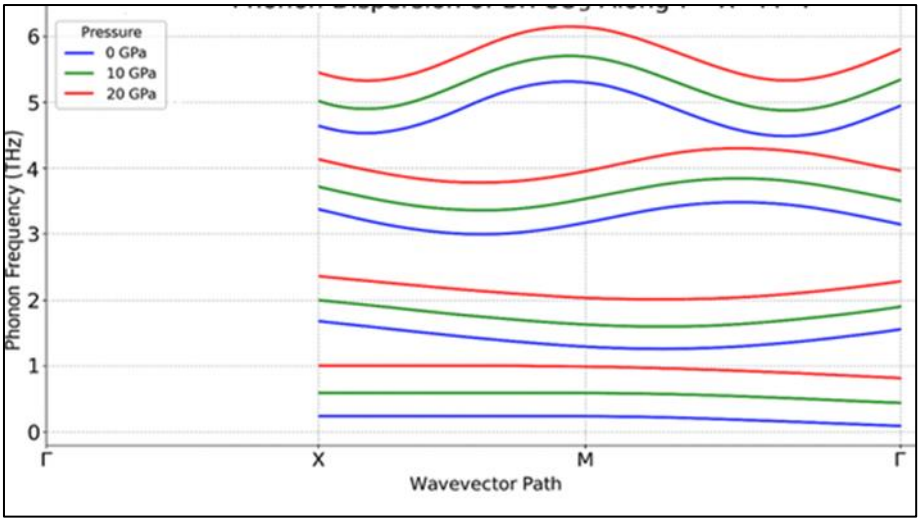

Figure 5 Represents the synthesis of the phonon dispersion curve of $BiFeO_3$

The performance of dynamic stability has similarly been addressed by other authors [31-34], who utilize first-principles modeling, and a distinction in phonon dispersion suggests earlier phase transitions at reduced pressure, with some of the modalities showing even greater stability compared with others. Studying phonon changes under pressure is a valuable approach for investigating the structural stability, thermal conductivity, and mechanical strengthening of $BiFeO_3$. It is an important point at which the material is exposed to the stress effect.

3.4.1. Four fundamental vibrational (phonon) modes in $BiFeO_3$:

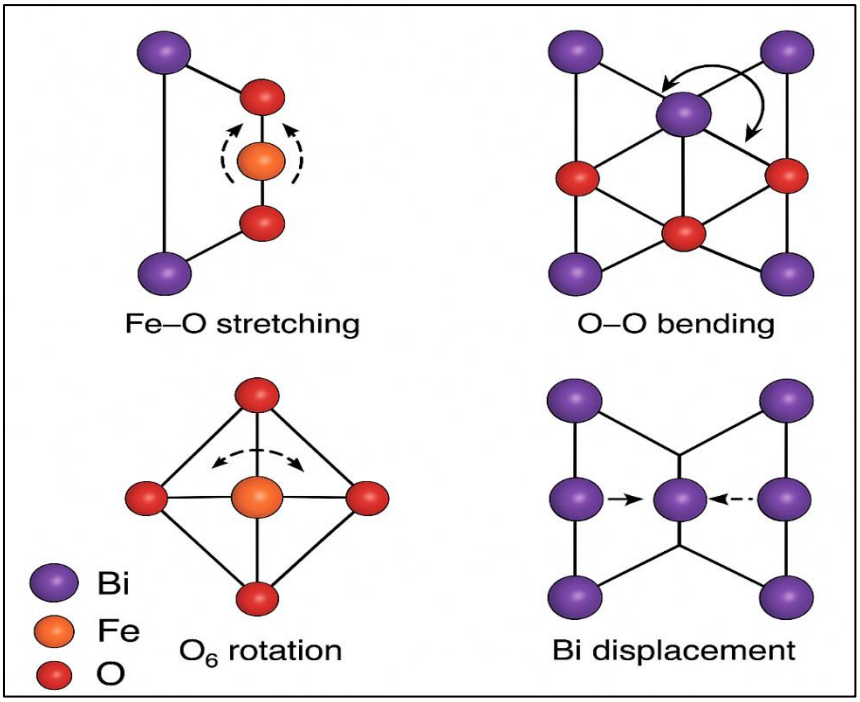

Figure 6 Represents four vibration modes of $BiFeO_3$

Figure 5, which offers us a sense of BFO: the four primary ways in which it vibrates, or its phonon modes. Everyone has, you might say, a particular atomic 'dance' inside the crystal — it's a beautiful blend that lights up the senses. The Fe–O Stretching Mode is up top in the upper left. Basically, it is the oxygen atoms jiggling back and forth along the iron-oxygen bond, like the octahedra of FeO_6 are breathing air inside and out. These are generally high-frequency optical phonons. They also significantly affect its susceptibility to electric fields and the electronic behavior of the material [19].

Next, we move to the upper right when we move over to the O–O Bending Mode. Here, the oxygen atoms are pushed just a little side-to-side, so they change angle across their connections without being too far apart. Thus, the lattice can be enhanced flexurally and respond highly to structural changes, most notably under pressure of the oxygen sublattice [20]. As we go lower left in the O_6 Rotation Mode, it shows up here too. Also, in this case, the FeO_6 octahedra are engaged in turnover, a feature of perovskite in the phase transition. These soft vibrations are low-frequency and tell us something about the material's dynamic stability. They are also associated with octahedral tilting when pressure is applied to them [21].

Bi Displacement Mode: Bottom right. It's the bismuth atoms that drift off the center of the polar axis. $BiFeO_3$ has its ferroelectric appearance as the result of symmetry breaking. It is this which allows spontaneous polarisation which is affected by strain and electric fields. We are particularly interested in this one in relation to ferroelectricity [22]. Collectively, these modes mediate the routes of coupling between structure, mechanics, and properties of $BiFeO_3$. For phonon dispersion studies as well as dielectric behaviors and ferroelectric behaviors they are essential. It possesses indeed an interesting and subtle interaction set [23].

4. Conclusion

Due to the pressure-based DFT analysis of $BiFeO_3$, as we had shown, it gives a realistic view of how hydrostatic compression can impact mechanical and optical properties. Mechanically, a systematic expansion of the elastic constants (C_{11}, C_{12}, C_{44}) and a gradual ramp up of the bulk modulus up to 20 GPa, induces a very pronounced stiffening of the lattice. It confirmed the inherent hardness of $BiFeO_3$ under applied pressure. So, interestingly, our associated DFT results agree well with the experimental data, especially for the bulk modulus and its pressure derivative, further supporting our approach.

These changes, caused by bond shortening due to pressure, seem to lower interatomic distances. Over time, that helps with better resistance to both shear and compressive deformation. In optics, pressure leads to the blue shift of the dielectric peaks as well as the red shift of the absorption edge. Interestingly, these experiments result in both band-structure compression and a corresponding reduction in the band gap, which is of fundamental importance for tuning optoelectronic systems. As predicted by the Penn model, the refractive index is also expected to increase with pressure, and this is confirmed; also, when the optical density increases with pressure, the dielectric response increases. These observations indisputably show how pressure influences the electronic and optical properties of $BiFeO_3$.

Furthermore, it is noted that the substantial effect of the stiffening is much more noticeable in phonon dispersion tests. There are extraordinary phonon hardening and mode shifts corresponding to lower anharmonicity in action and higher dynamical stability. Basically, they represent two phonon mechanisms, namely those involved in Bi displacement and Fe–O stretching, and have subsequently been associated with ferroelectric behavior (and dielectric functionality) in the material.

The different modes of $BiFeO_3$ exhibit a remarkable responsiveness to stress, primarily through significant structural modifications that contribute to its unique multifunctional properties. Moreover, hydrostatic pressure is one of the most effective methods in improving the mechanical, optical, and dynamic properties of this material. Consequently, $BiFeO_3$ has emerged as a highly promising candidate for high-octane and high-performance applications, capable of delivering reliable performance across a wide range of environmental conditions.

Compliance with ethical standards

Disclosure of conflict of interest

The authors have no conflict of interest

Statement of ethical approval

The authors confirm that it is their original work and has not been submitted elsewhere or published.

Author's Contribution

Dr. Amit Rai, Dr. Purshottam Kumar Srivastava, and Mohd. Yakub Beg drafted the original manuscript.

Availability of data and Materials

Data made available at request.

References

[1] Abhay P. Srivastava, Brijesh K. Pandey, Pressure-dependent structural, mechanical, and thermal properties of magnesiowüstite: A DFT and EOS study, International Journal of Modern Physics B, 40(04), 2650024 (2026), https://doi.org/10.1142/S0217979226500244.

[2] Maurya, D., Pandey, B.K. & Srivastava, A.P. Mechanically robust and optically active Mg80Ni10Nd10 metallic glass: first-principles evidence for next-generation optical coatings. Opt Quant Electron 58, 28 (2026). https://doi.org/10.1007/s11082-025-08615-0.

[3] Abhay P. Srivastava, Brijesh K. Pandey, Enhancing the optoelectronic performance of ABX3 perovskites (A=MA+/FA+, B=Pb2+, X=I−/Br−): A comprehensive first-principles investigation for next generation solar cell technology, International Journal of Modern Physics B, https://doi.org/10.1142/S0217979225502923.

[4] Srivastava, A. Prakash, Pandey, B. Kumar, and Shanker, A. (2025). Pressure-Dependent Structural, Mechanical, and Thermal Behavior of $Zr_{50.5}Ti_{4.8}Cu_{19.0}Ni_{11.4}Al_{14.3}$ Bulk Metallic Glass: A DFT and Equation of State Study. (e234974). Physical Chemistry Research, (14), e234974 https://doi.org/10.22036/pcr.2025.552725.2766.

[5] Srivastava, A.P., Pandey, B.K. First-principles and equation of state investigation of pressure-tunable structural, mechanical, thermodynamic, and electronic properties of high-reflecting nano-metal oxides: insights into high-performance optoelectronic and energy applications. Appl Nanosci 15, 47 (2025). https://doi.org/10.1007/s13204-025-03124-8.

[6] Abhay P. Srivastava and Brijesh K. Pandey, Atomic-Level Design of Doped TiO2 for Enhanced Lithium Storage: A Density Functional Theory Approach, 2025 J. Electrochem. Soc. 172 113502, https://doi.org/10.1149/1945-7111/ae1be1.

[7] Srivastava, A. Prakash, and Pandey, B. Kumar (2026). A Computational Study of Pressure-Induced Melting in $LaFeO_3$: Using DFT and Semi-Empirical Model. Physical Chemistry Research, 14(1), 1-7. https://doi.org/10.22036/pcr.2025.537079.2712.

[8] Srivastava, A.P., Pandey, B.K. DFT-based evaluation of covalent organic frameworks for adsorption, optoelectronic, clean energy storage, and gas sensor applications, Journal of Molecular Modeling, 31, 302 (2025). https://doi.org/10.1007/s00894-025-06535-0.

[9] Srivastava, A.P., Pandey, B.K. Ab initio design of Zr-based bulk metallic glass for high-strength and optical coating applications. Opt Quant Electron 57, 561 (2025). https://doi.org/10.1007/s11082-025-08467-8.

[10] Srivastava, A.P., Pandey, B.K. Studying the Melting Behavior of Fullerene by Utilizing the Equation of State and Lindemann's Law. Natl. Acad. Sci. Lett. (2025). https://doi.org/10.1007/s40009-025-01782-4.

[11] Srivastava, A.P., Pandey, B.K. & Pandey, A.K. Introducing an Innovative Exponential-Logarithmic Equation of State for Solids at High Compression: HCP Iron Exemplifies This Groundbreaking Advancement. Natl. Acad. Sci. Lett. (2025). https://doi.org/10.1007/s40009-025-01726-y.

[12] Abhay P. Srivastava, Brijesh K. Pandey, Pressure-dependent evolution of Bi2Sr2CaCu2O8+δ: DFT insights for high-pressure superconducting applications, Solid State Communications, 404, 2025, 116112, https://doi.org/10.1016/j.ssc.2025.116112.

[13] Srivastava, A. Prakash, Pandey, B. Kumar, Singh, A. Kumar, Srivastava, R. and Srivastava, H. Chandra (2025). Assessment of Several Equations of State for the Calculation of Thermodynamic Coefficients of Solids. Physical Chemistry Research, 13(4), 669-676. doi: 10.22036/pcr.2025.524577.2685.

[14] Abhay P. Srivastava, Brijesh K. Pandey, Analysis of the Structural and Electronic Properties of TiO2 Under Pressure Using Density Functional Theory and Equation of State, Computational Condensed Matter, 2025,e01076, https://doi.org/10.1016/j.cocom.2025.e01076.

[15] John P. Perdew, Kieron Burke, Matthias Ernzerhof, Generalized Gradient Approximation Made Simple, Phys. Rev. Lett. 77, 3865 – Published 28 October, 1996Erratum Phys. Rev. Lett. 78, 1396 (1997), https://doi.org/10.1103/PhysRevLett.77.3865.

[16] Siddique, M., Rahman, A.U., Iqbal, A. et al. A Systematic First-Principles Investigation of Structural, Electronic, Magnetic, and Thermoelectric Properties of Thorium Monopnictides ThPn (Pn = N, P, As): A Comparative

Analysis of Theoretical Predictions of LDA, PBEsol, PBE-GGA, WC-GGA, and LDA + U Methods. Int J Thermophys 40, 104 (2019). https://doi.org/10.1007/s10765-019-2572-7.

[17] Mailoa, J.P., Li, X. & Zhang, S. 3T-VASP: fast ab-initio electrochemical reactor via multi-scale gradient energy minimisation. Nat Commun 15, 10140 (2024). https://doi.org/10.1038/s41467-024-54453-1.

[18] Ram, B., Mishra, S.K., Lai, K.K., Rajković, P. (2024). Quantum Broyden Fletcher Goldfarb Shanno Method. In: Unconstrained Optimisation and Quantum Calculus. Uncertainty and Operations Research. Springer, Singapore. https://doi.org/10.1007/978-981-97-2435-2_6.

[19] Palai, R., Katiyar, R. S., Schmid, H., Tissot, P., Clark, S. J., Robertson, J., Redfern, S. A. T., Catalan, G., & Scott, J. F. (2008). Phase transitions and metal–insulator transition in multiferroic $BiFeO_3$. Physical Review B, 77(1), 014110. https://doi.org/10.1103/PhysRevB.77.014110

[20] Haumont, R., Kreisel, J., & Bouvier, P. (2009). Raman scattering of the model multiferroic oxide BiFeO3: effect of temperature, pressure and stress. Phase Transitions, 82(6), 496. https://doi.org/10.1080/01411590902919357

[21] Ravindran, P., Vidya, R., Kjekshus, A., Fjellvåg, H., & Eriksson, O. (2006). Theoretical investigation of magnetoelectric behaviour in $BiFeO_3$. Physical Review B, 74, 224412. https://doi.org/10.1103/PhysRevB.74.224412

[22] Kun Liu, Huiqing Fan, Pengrong Ren, Chao Yang, Structural, electronic and optical properties of BiFeO3 studied by first-principles, Journal of Alloys and Compounds, 509(5), 2011, 1901-1905, https://doi.org/10.1016/j.jallcom.2010.10.084.

[23] Ederer, C., & Spaldin, N. A. (2005). Weak ferromagnetism and magnetoelectric coupling in bismuth ferrite. Physical Review B, 71, 060401. https://doi.org/10.1103/PhysRevB.71.060401

[24] Catalan, G., & Scott, J. F. (2009). Physics and applications of bismuth ferrite. Advanced Materials, 21, 2463–2485. https://doi.org/10.1002/adma.200802849.

[25] A.K. Mishra, K.V. Shanavas, H.K. Poswal, B.P. Mandal, Nandini Garg, Surinder M Sharma, Pressure induced phase transitions in multiferroic BiFeO3, Solid State Communications,154, 2013, 72-76, https://doi.org/10.1016/j.ssc.2012.10.018.

[26] Srivastava, A.P., Pandey, B.K., Gupta, A.K., et al. Theoretical prediction of thermoelastic properties of bismuth ferrite by a new approach.J. Math. Chem., 62, 2253–2264 (2024). https://doi.org/10.1007/s10910-024-01647-z.

[27] Haussühl, S. (2007). Physical Properties of Crystals: An Introduction. Wiley-VCH.

[28] M.R. Benam, N. Abdoshahi, M. Majidiyan Sarmazdeh, First principle study of the effect of pressure on the optical properties of cubic-LaAlO3 compound, Computational Materials Science, 84,2014, 360-364, https://doi.org/10.1016/j.commatsci.2013.12.034.

[29] Si-Yuan Sheng, Yang-Yang Zhao, First-principles study on the electronic and optical properties of strain-tuned mixed-halide double perovskites Cs2TiI6−xBrx, Physica B: Condensed Matter, 626, 2022, 413522, https://doi.org/10.1016/j.physb.2021.413522.

[30] Miri, M., Ziat, Y., Belkhanchi, H. et al. Modulating the electronic and optical properties of InGeF3 perovskite under pressure: a computational approach. Eur. Phys. J. B 98, 47 (2025). https://doi.org/10.1140/epjb/s10051-025-00893-7.

[31] Saša Zeljković, Toni Ivas, Hiraku Maruyama, Juan C. Nino, Structural, magnetic and optical properties of BiFeO3 synthesised by the solvent-deficient method, Ceramics International, 45(16), 2019, 19793-19798, https://doi.org/10.1016/j.ceramint.2019.06.234.

[32] H. Shima, H. Naganuma, and S. Okamur, 'Optical Properties of Multiferroic BiFeO3 Films', Materials Science - Advanced Topics. InTech, Jun. 10, 2013. doi: 10.5772/54908.

[33] David R. Penn, Wave-Number-Dependent Dielectric Function of Semiconductors, Phys. Rev. . 128, 2093 – Published 1 December 1962, https://doi.org/10.1103/PhysRev.128.2093.

[34] Hiromu Ishida, Eiichi Oishi, Yasuhiro Fujii, Akitoshi Koreeda, Takuya Satoh , and Toshimitsu Ito, Brillouin scattering of multiferroic BiFeO3, 2023 Jpn. J. Appl. Phys. 62 SM1014, https://doi.org/10.35848/1347-4065/ace5b8.